

Condensation of Forced Convection Two-Phase Flow in a Miniature Tube

E. BEGG¹, A. FAGHRI¹, ¹ *Department of Mechanical Engineering, University of Connecticut, Storrs, CT 06269*, D. KRUSTALEV², ² *Thermocore, Inc. Lancaster, PA 17601*

Nomenclature

c_p	specific heat at constant pressure, J/(kg-K)
f_v	vapor friction factor
h_{fg}	latent heat of vaporization, J/kg
h_o	outer surface convective heat transfer coefficient, W/(m ² K)
k	thermal conductivity, W/(m-K)
L_δ	length of the liquid film to the point of complete condensation (Fig. 1), m
K	curvature, m ⁻¹
Ma	$\bar{w}_v / \sqrt{\gamma_0 R_g T_v}$, Mach number
$\dot{m}_{l,in}$	liquid mass flow rate at $z = 0$, kg/s
\dot{m}_l	total mass flow rate at $z = 0$, kg/s
\dot{m}	mass flow rate, kg/s
p	pressure, Pa
Q	$Q = 2\pi R \int_0^z q_w dz - (c_{p,l} \dot{m}_l \bar{T}_l - c_{p,l,in} \dot{m}_{l,in} \bar{T}_{l,in})$, axial heat flow due to phase change, W
q	heat flux, W/m ²
r	radial coordinate, m
R	inner radius of the channel, m
R_g	gas constant, J/(kg-K)
Re	$2\bar{w}_v (R - \delta) \rho_v / \mu_v$, axial vapor Reynolds number
Re_r	$2v_{v,\delta} (R - \delta) \rho_v / \mu_v$, radial vapor Reynolds number
T	temperature, K
v	radial velocity, m/s
w	axial velocity, m/s
\bar{w}	area-averaged axial velocity m/s
z	axial coordinate, m

Greek Symbols

α	accommodation coefficient
β	momentum flux coefficient
γ_0	c_p/c_v , ratio of specific heats
Δ	$d\delta/dz$
δ	liquid film thickness, m
μ	dynamic viscosity, Pa-s
ρ	density, kg/m ³
σ	surface tension, N/m
φ	inclination angle

Subscripts

ent	entrance
in	at $z = 0$
l	liquid
men	meniscus
sat	saturation
v	vapor
w	wall
δ	liquid film free surface
$crit$	at critical complete condensation

Introduction

Electronic cooling and other high heat flux applications require a fundamental understanding of the condensation process in small diameter channels in order to optimize design configurations of devices used in these applications. Unlike conventional size passages in which surface tension effects are limited, surface tension in miniature size channels can have a significant role on the overall hydrodynamics and in particular on the thin films that are believed to be the dominant mechanisms controlling the heat transfer characteristics.

For forced convection condensation in miniature circular tubes the two phase flow regime maps for conventional sized tubes may not be relevant because of the role of surface tension in the hydrodynamics. Srinivasan and Shah (1997) point out that very limited data is available concerning the basic flow patterns for two phase flow with or without heat transfer in miniature circular tubes.

Condensation in conventional size circular tubes comprise a well-defined body of work. Collier and Thome (1994) present a generally accepted description of the two phase flow patterns during forced convection condensation in conventional size horizontal tubes with co-current flow. The range of flow patterns present depend on the total energy convected into the tube. In order of increasing velocity, the flow is found to be stratified, slug, plug or wavy, and annular.

The objective of this work is to model annular film condensation in miniature circular cylinder tubes where capillary phenomena can conceivably result in blocking of the tube cross section with liquid at some distance from the condenser entrance. A physical description is illustrated in Fig. 1 (a). This phenomenon is referred to as complete condensation. An experiment with visualization was conducted and a mathematical

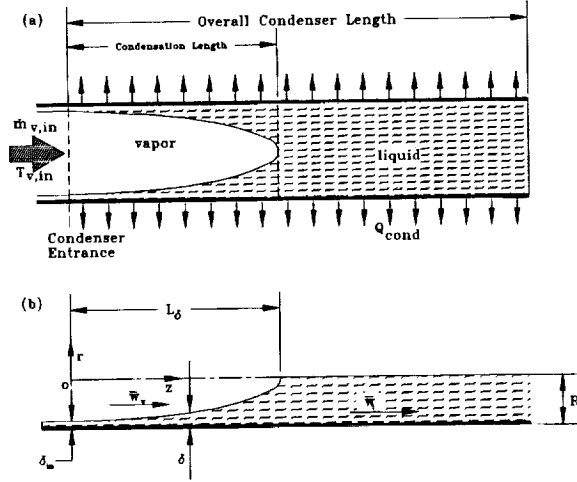


Figure 1: Description of the physical model for annular film condensation in a miniature tube. (a) Structure of two phase flow for complete condensation. (b) Coordinate system and conventions for film condensation model.

model was developed on this subject in this work.

Flow Visualization in Miniature Tubes

A circular Pyrex tube of 3.25 mm inside diameter and 5.00 mm outside diameter was used in a loop thermosyphon for flow visualization. The overall length of the horizontal test section was 302 mm with an insulated inlet section of 97 mm and a condenser length of 205 mm. Experiments were conducted over a range of heat loads from 4.9 to 10 W.

Figure 2 is a photograph of the complete condensation phenomenon for the operating conditions of $Q_{in} = 7.7W$, $T_v = 59.0^\circ C$. A liquid film on the lower wall is obvious closer to the location of complete condensation. A dramatic thinning of the film on the lower wall is also apparent. Immediately after the decrease in film thickness at the bottom wall, the liquid is seen to completely span the tube cross section. The closing off of the channel to vapor flow appears similar to a capillary tube meniscus. Note the slight inclination of the meniscus due to the effect of gravity.

Mathematical Formulation

A summary of the analysis is given below. For the complete development of the mathematical model see Begg et al. (1998).

A steady state mathematical model of condensation which leads to complete condensation is presented and includes cou-

pled vapor and liquid flows with shear stresses at the liquid free surface due to the vapor-liquid frictional interaction and surface tension gradient. The model is based on the following simplifying assumptions:

1. The vapor is saturated and there is no temperature gradient in vapor in radial direction.
2. Heat transport in the thin liquid films is only due to conduction in the radial direction.
3. Inertia terms can be neglected for the viscous flow in the liquid films with low Reynolds numbers.
4. Force on liquid due to surface tension is much greater than the gravitational force and therefore the liquid is distributed onto the walls in a film of locally uniform thickness.
5. The solid tube wall is infinitely thin so that its thermal resistance in the radial direction can be neglected as well as the axial heat conduction.

The cylindrical coordinate system used is shown in Fig. 1(b). Both the vapor and liquid flow along the z -coordinate. The physical situation should be described taking into consideration the vapor compressibility and the vapor temperature variation along the channel. Also the second principal radius of curvature of the liquid-vapor interface should be accounted for (in the equation relating vapor and liquid pressures) while it is usually neglected in modeling of film flows in tubes of larger diameters. The mass and energy balances for the liquid film shown in Fig. 2(a) yield:

$$\frac{dQ}{dz} = 2\pi k_t \frac{T_w - T_\delta}{\ln[R/(R - \delta)]} - \frac{d}{dz} (c_{p,\ell} \dot{m}_\ell \bar{T}_\ell) \quad (1)$$

where \bar{T}_ℓ is the area-averaged liquid temperature for a given z location. For consideration of subcooling in the condensed liquid, \bar{T}_ℓ is found from an average area given by

$$\bar{T}_\ell = \frac{2 \int_{R-\delta}^R r T_\ell(r) dr}{[R^2 - (R - \delta)^2]} \quad (2)$$

where $T_\ell(r)$ is the assumed liquid film temperature profile given by the temperature distribution in a cylindrical wall.

$$T_\ell(r) = T_\delta + \frac{T_w - T_\delta}{\ln \frac{R}{R-\delta}} \ln \frac{r}{R-\delta} \quad (3)$$

The derivative of \bar{T}_ℓ is approximated by

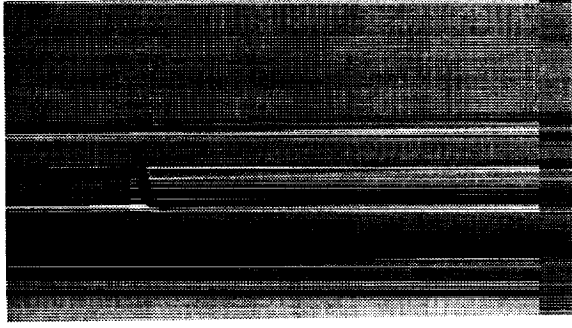


Figure 2: Photograph of annular film condensation resulting in complete condensation in a 3.25 mm inside diameter tube. $Q_{in} = 7.7W$, $T_v = 59.0^\circ C$

$$\frac{dT_l}{dz} = \frac{dT_\delta}{dz} + \left(\frac{dT_w}{dz} - \frac{dT_\delta}{dz} \right) \times \ln \left(\frac{R-\delta}{R} \right) \frac{2}{[R^2 - (R-\delta)^2]} \left[\left(\ln \frac{R}{R-\delta} - \frac{1}{2} \right) \frac{R^2}{2} + \frac{(R-\delta)^2}{4} \right] \quad (4)$$

The momentum conservation for viscous flow in a liquid film in which the inertia terms are assumed to be negligible is

$$\frac{1}{r} \frac{\partial}{\partial r} \left(r \frac{\partial w_l}{\partial r} \right) = \frac{1}{\mu_l} \left(\frac{dp_l}{dz} + \rho_l g \sin \varphi \right) \quad (5)$$

The boundary conditions for the last equation are the non-slip condition at $r = R$ and specified shear stresses at the liquid-vapor interface due to the frictional liquid-vapor interaction, $\tau_{l,v}$, and the surface tension gradient related to the interfacial temperature gradient along the channel.

$$w_l|_{r=R} = 0 \quad (6)$$

$$\frac{\partial w_l}{\partial r} \Big|_{(r=R-\delta)} = \frac{1}{\mu_l} \left[-\tau_{l,v} - \frac{d\sigma}{dT} \frac{dT_\delta}{dz} \right] \equiv E \quad (7)$$

where T_δ is the local liquid-vapor interface temperature and $\frac{d\sigma}{dT}$ is the Marangoni effect.

Taking into account the effect of the condensation process on the shear stress term, an expression from the Munoz-Cobol et al. (1996) analysis is used for $\tau_{l,v}$. The equation for the axial pressure gradient in the liquid is

$$\frac{dp_l}{dz} = \rho_l g \sin \varphi + \mu_l \left[\frac{1}{2\pi\rho_l} \left(\frac{Q}{h_{fg}} - \dot{m}_{l,in} \right) + E(R-\delta)F \right]$$

$$\left[\frac{R^4}{16} + \frac{(R-\delta)^2}{2} \left(F + \frac{(R-\delta)^2}{8} - \frac{R^2}{4} \right) \right]^{-1} \quad (8)$$

where

$$F = \frac{(R-\delta)^2}{2} \left(\ln \frac{R}{R-\delta} + \frac{1}{2} \right) - \frac{R^2}{4} \quad (9)$$

The pressure difference between the vapor and liquid phases is due to capillary effects (Faghri, 1995).

$$p_v - p_l = \sigma \left\{ \frac{d^2\delta}{dz^2} \left[1 + \left(\frac{d\delta}{dz} \right)^2 \right]^{-3/2} + \frac{1}{R-\delta} \cos \left(\text{atan} \frac{d\delta}{dz} \right) \right\} - p_d \quad (10)$$

The term with cosine in the right-hand side of this equation is due to the second principal radius of the interfacial curvature for a cylindrical film. Introducing an additional variable

$$d\delta/dz = \Delta \quad (11)$$

eq. (10) can be rewritten as follows.

$$\frac{d\Delta}{dz} = [1 + (\Delta)^2]^{3/2} \left(\frac{p_v - p_l + p_d}{\sigma} - \frac{\cos(\text{atan}\Delta)}{R-\delta} \right) \quad (12)$$

The compressible quasi-one-dimensional momentum equation for the vapor flow in the form suggested by Bankston and Smith (1973) is modified to account for non-uniformity of the vapor cross-sectional area of the liquid-vapor interface following Faghri (1995).

$$\frac{dp_v}{dz} = \rho_v g \sin \varphi + \frac{1}{A_v} \left[\frac{d}{dz} (-\beta_v \rho_v \bar{w}_v^2 A_v) - f_v \rho_v \bar{w}_v^2 \pi (R-\delta) + 2\pi (R-\delta) \rho_v v_{v,\delta}^2 \sin(\text{atan}\Delta) \right] \quad (13)$$

with $\beta_v = 1.33$ for small radial Reynolds numbers.

The perfect gas law is employed to account for the compressibility of the vapor

$$\rho_v = \frac{p_v}{R_g T_v} \quad (14)$$

Therefore

$$\frac{d\rho_v}{dz} = \frac{1}{R_g} \left(\frac{dp_v}{dz} \frac{1}{T_v} - \frac{p_v}{T_v^2} \frac{dT_v}{dz} \right) \quad (15)$$

The saturated vapor temperature and pressure are related by the Clausius-Clapeyron equation which can be written in the following form.

$$\frac{dT_v}{dz} = \frac{dp_v}{dz} \frac{R_g T_v^2}{p_v h_{fg}} \quad (16)$$

The seven first order differential equations Eqs. (1), (8), (11), (12), (13), (15), and (16) include the following seven variables: δ , Δ , p_t , Q , p_v , ρ_v , and T_v . Therefore, seven boundary conditions are set forth at $z = 0$

$$\delta = \delta_{in} \quad (17)$$

$$\Delta = 0 \quad (18)$$

$$p_t = p_{v,in} - \frac{2\sigma}{R - \delta_{in}} + p_d \quad (19)$$

$$Q = 0 \quad (20)$$

$$p_v = p_{v,in} = p_{v,sat}(T_{v,in}) \quad (21)$$

$$\rho_{v,in} = \frac{p_{v,in}}{R_g T_{v,in}} \quad (22)$$

$$T_v = T_{v,in} \quad (23)$$

In boundary condition (17), δ_{in} is defined from the condition in the adiabatic zone at the entrance to the condenser where the liquid and vapor pressure gradients are equal. This condition is satisfied by solving equations (8) and (13) for δ_{in} for the case of $Q = 0$, $v_{v,\delta} = 0$, $dA_v/dz = 0$ and $dT_\delta/dz = 0$. There are also parameters $\dot{m}_{t,in}$ and $\bar{w}_{v,in}$ and an additional variable T_δ involved in this problem. They will be considered using additional algebraic equations. The parameter $\dot{m}_{t,in}$ should be found using a constitutive condition at the entrance of the condenser.

$$\dot{m}_{t,in} = \dot{m}_t - Q_t/h_{fg} \quad (24)$$

where Q_t is the total heat load of the condenser. Also $\bar{w}_{v,in} = Q_t/(h_{fg}\rho_v A_{v,in})$.

The liquid-vapor interface temperature, T_δ , differs from the saturated bulk vapor temperature because of the interfacial resistance and effects of curvature on saturation pressure over liquid films. The interfacial resistance, is defined as (Faghri, 1995):

$$q_\delta = - \left(\frac{2\alpha}{2 - \alpha} \right) \frac{h_{fg}}{\sqrt{2\pi R_g}} \left[\frac{p_v}{\sqrt{T_v}} - \frac{(p_{sat})_\delta}{\sqrt{T_\delta}} \right] \quad (25)$$

where p_v and $(p_{sat})_\delta$ are the saturation pressures corresponding to T_v and at the thin liquid film interface, respectively.

The following two algebraic equations should be solved to determine T_δ for every point along the z -direction. The relation between the saturation vapor pressure over the thin evaporating film, $(p_{sat})_\delta$, affected by the surface tension, and the normal saturation pressure corresponding to T_δ , $p_{sat}(T_\delta)$, is given by the extended Kelvin equation (Faghri, 1995):

$$(p_{sat})_\delta = p_{sat}(T_\delta) \exp \left[\frac{(p_{sat})_\delta - p_{sat}(T_\delta) - \sigma K + p_d}{\rho_t R_g T_\delta} \right] \quad (26)$$

where K is the local curvature of the liquid-vapor interface defined by the term in outer brackets in eq. (10). Noticing that under steady state conditions, q_δ is due to heat conduction through the liquid film, it follows from this condition and eq. (25):

$$T_\delta = T_w + \frac{(R - \delta)}{k_t} \ln \frac{R}{R - \delta} \left(\frac{2\alpha}{2 - \alpha} \right) \frac{h_{fg}}{\sqrt{2\pi R_g}} \left[\frac{p_v}{\sqrt{T_v}} - \frac{(p_{sat})_\delta}{\sqrt{T_\delta}} \right] \quad (27)$$

Equations (26) and (27) determine the interfacial temperature, T_δ , and pressure, $(p_{sat})_\delta$, for a given vapor pressure, $p_v = p_{v,sat}(T_v)$, temperature of the solid-liquid interface, T_w , and the liquid film thickness, δ .

For the case of variable wall temperature, an additional variable, T_w , and first order ordinary differential equation must be added to the seven previously specified.

T_w is local wall temperature and can vary along the condenser length. If the convective heat transfer coefficient at the outer tube wall, h_o and the cooling liquid temperature, T_∞ , are known, the local wall temperature can be defined using an energy balance.

$$h_o(T_w - T_\infty) = \frac{1}{2\pi R} \frac{dQ}{dz} \quad (28)$$

Another boundary condition is also required and that is given by

$$z = 0, T_w = T_{w,in} \quad (29)$$

Numerical Procedure

Equations (1), (8), (13), (15), and (16) with corresponding boundary conditions have been solved using the standard Runge-Kutta procedure. Algebraic equations (26) and (27) with two unknowns, $(p_{sat})_\delta$ and T_δ , have been solved numerically for every point on z using a standard numerical procedure

(Wegstein's iteration method). All the unknown variables were found with the accuracy of 0.0005%. During the numerical procedure the interval $0 \leq z \leq L_\delta$ was divided into at least 500 parts, and the thermophysical properties of the saturated vapor and liquid were recalculated for each of the parts at the corresponding vapor temperature $T_v(z)$.

Results and Discussion

Figure 3 (a) shows variation of the liquid film thickness along the condenser with a constant wall temperature of 340 K. The vapor ($T_{v,in} = 363$ K) pressure drop over the condensation length is insignificant compared to the liquid pressure drop as shown in Figs. 3 (b, c). Condensation is more intensive in the region where the film thickness is at the minimum. For the cases of $Q_{in} = 8$ W and $Q_{in} = 10$ W, representing complete condensation and critical complete condensation, respectively, the incoming vapor is totally condensed. This is not true for $Q_{in} = 12$ W, the incomplete condensation case. Figure 3 (d) shows the cumulative sum of the heat removed from the vapor by condensation. For $Q_{in} = 12$ W, not all of the heat load coming into the condenser is rejected at the termination of the calculation.

Results are obtained for the convective cooling boundary condition shown in Fig. 4. The wall temperature is non-uniform with a significant increase just prior to the point of complete condensation, coincident with the thinning of the liquid film, as shown in Fig. 4 (d). Decrease of the convective heat transfer coefficient, h_o , from 20,000 to 15,000 $\text{W/m}^2\text{K}$ resulted in an increase of the wall temperature that shortened the condensation length, as shown in Fig. 4 (a, d).

Summary of the Complete Condensation Phenomenon

Features of complete condensation in the annular film regime include the segregation of liquid and vapor into distinct regions within the tube. Initially, the annular film thickness increases gradually in the downstream direction. After reaching the local maximum value, it suddenly decreases to its minimum thickness and then dramatically increases to the radius of the tube. The region at the convergence of the liquid film is similar to the classic capillary meniscus in appearance. This forms a well defined location marking the transition to single-phase liquid flow. Downstream of the location of the meniscus-like surface, the entire cross section of the tube is occupied by liquid. Any additional heat removal downstream of this location only results in subcooling of the liquid. The axial distance from the inlet of the condenser tube at $z = 0$ to the location at which the entire cross section is filled with liquid is defined as L_δ , the condensation length.

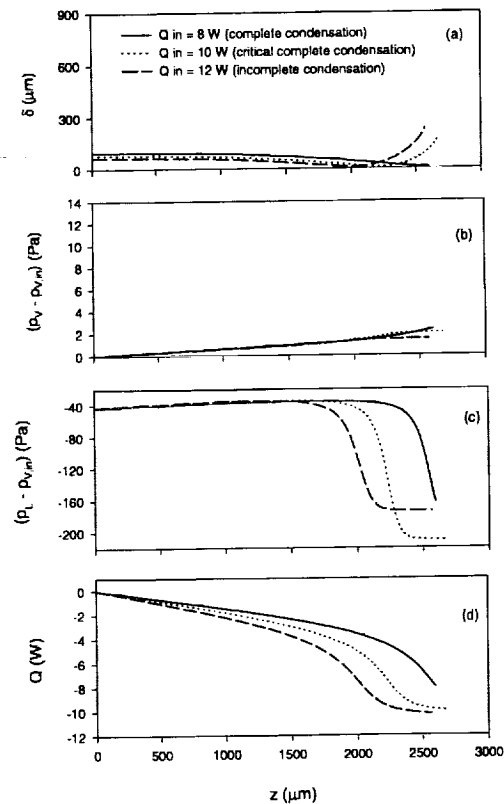


Figure 3: Annular film condensation in circular tube with constant wall temperature. $R = 1.5\text{mm}$, $m_t = 0.01\text{g/s}$, $T_w = 340\text{K}$, $T_v = 363\text{K}$ (a) film thickness (b) vapor pressure (c) liquid pressure (d) cumulative heat rate rejected

Conclusions

Based on the numerical results and visual observations, the following conclusions have been made.

1. Length of film condensation in miniature tubes is very restricted due to surface tension effects that result in complete condensation a short distance from the condenser inlet.
2. The complete condensation length is a non-linear function of the vapor-wall temperature difference, increasing with the temperature difference approaching zero.
3. Pressure drop in the vapor phase was usually insignificant compared to the pressure drop in liquid. Consequently, the vapor temperature variation along the condenser was infinitesimal.
4. Variation of the wall temperature can be significant for convective cooling boundary condition.
5. Complete condensation in small diameter tubes is a truly steady phenomenon.

A very distinct transition is anticipated between the steady phenomenon of complete condensation and the next two-phase flow regime, which is referred to here as incomplete condensation. It is anticipated that incomplete condensation will be characterized by fluctuations of the liquid-vapor interface in the annular film which result in bubbles of vapor passing downstream of confluence of the liquid film. The meniscus-like feature will no longer be stationary and an unsteady two-phase flow bubbly-type flow will exist in the tube.

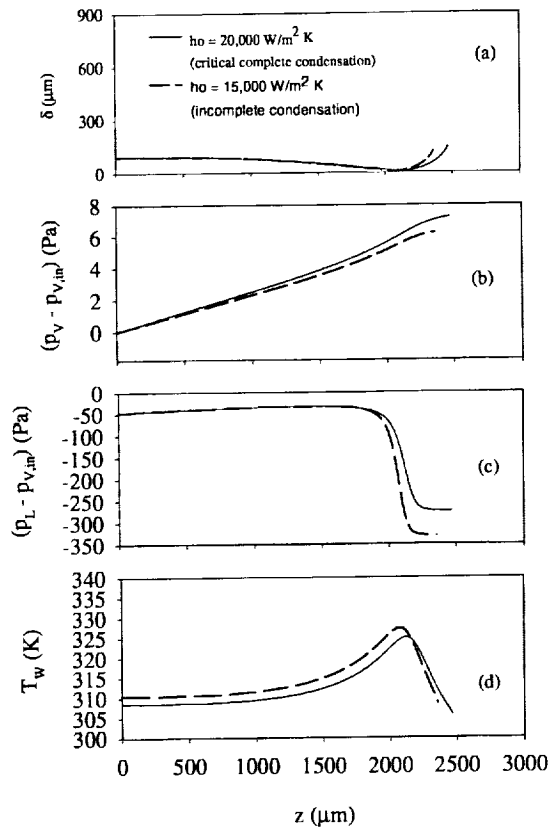


Figure 4: Annular film condensation in circular tube with convective boundary condition. $R = 1.5\text{mm}$, $m_t = 0.01\text{g/s}$, $T_{v,in} = 323\text{K}$, $T_{inf} = 300\text{K}$, $Q_{in} = 5.83\text{W}$
 (a) film thickness (b) vapor pressure (c) liquid pressure (d) wall temperature

Acknowledgments

Funding for this work was provided by NASA Grant NAG3-1870 and NSF Grant CTS-941458.

References

- Begg, E., Khrustalev, D., and Faghri, A., "Complete Condensation of Forced Convection Two Phase Flow in a Miniature Tube," to be presented at ASME International Conference, Anaheim, CA. Nov. 1998.
- Bankston, C.A. and Smith, H.J., 1973, "Vapor Flow in Cylindrical Heat Pipes," ASME J. Heat Transfer, Vol.95, pp. 371-376.
- Collier, J. G. and Thome, J. R., 1994, Convective Boiling and Condensation, Third Edition, Oxford University Press, New York.

Faghri, A., 1995 Heat Pipe Science and Technology, Taylor and Francis, Washington, D.C.

Munoz-Cobo, J.L., Herranz, L., Sancho, J., Tkachenko, I., and Verdu, G., 1996, "Turbulent Vapor Condensation With Noncondensable Gases in Vertical Tubes," *Int. J. Heat Mass*

Transfer, Vol. 39, No. 15, pp. 3249 - 3260,.

Srinivasan, V. and Shah, R. K., 1997, "Condensation in Compact Heat Exchangers," *Enhanced Heat Transfer*, vol. 4, pp. 237-256.